Global datasets of hourly carbon and water fluxes simulated using a satellite-based process model with dynamic parameterizations

Responses to the comments on essd-2023-328 by Anonymous Referee #2

Jiye Leng et al.

The paragraphs in blue Italic indicate the corresponding revised paragraphs in the manuscript. The under-reviewed papers will be preprinted in the final manuscript before the publication.

1. Need particular explanation on the newly revised BEPS regarding how exactly the hourly GPP and ET were simulated but not from the previous version. If BEPS was designed to simulate the hourly products, were if just because the hourly inputs were not available before?

Thanks for the question. The newly revised BEPS v4.10 keeps the original structure and algorithms but with new standardized framework using the Doxygen format and Git version control. The name for BEPS was also revised from the former '*Boreal Ecosystem Productivity Simulator*' to '*Biosphere-atmosphere Exchange Process Simulator*'. We also open-sourced the BEPS model after the code standardization. BEPS adopts hourly meteorological variables to simulate carbon and water fluxes using the same algorithms in Chen et al. (2012). Besides, BEPS has been comprehensively evaluated in several site-level, showing its capacity to simulate gross primary productivity (GPP) and evapotranspiration (ET) comparable to the eddy covariance measurements (Gonsamo et al., 2013; Luo et al., 2018; Luo et al., 2019).

Due to the computational capacity and data volume, the global hourly GPP and ET dataset based on BEPS has not yet been published before. In this study, compared to the previous research papers on BEPS, we adopted dynamic parameterizations to improve the accuracy of simulated carbon and water fluxes, and presented and analyzed the global GPP and ET in 2001-2020 at the hourly timescale for the first time.

References:

Chen, J.M., Mo, G., Pisek, J., Liu, J., Deng, F., Ishizawa, M., & Chan, D. (2012). Effects of foliage clumping on the estimation of global terrestrial gross primary productivity. *Global Biogeochemical Cycles*, 26Gonsamo, A., Chen, J.M., Price, D.T., Kurz, W.A., Liu, J., Boisvenue, C., Hember, R.A., Wu, C., & Chang, K.-H. (2013). Improved assessment of gross and net primary productivity of Canada's landmass. *Journal of Geophysical Research: Biogeosciences*, 118, 1546-1560

Luo, X., Chen, J.M., Liu, J., Black, T.A., Croft, H., Staebler, R., He, L., Arain, M.A., Chen, B., Mo, G., Gonsamo, A., & McCaughey, H. (2018). Comparison of Big-Leaf, Two-Big-Leaf, and Two-Leaf Upscaling Schemes for Evapotranspiration Estimation Using Coupled Carbon-Water Modeling. *Journal of Geophysical Research: Biogeosciences*, 123, 207-225

Luo, X., Croft, H., Chen, J.M., He, L., & Keenan, T.F. (2019). Improved estimates of global terrestrial photosynthesis using information on leaf chlorophyll content. *Global Change Biology*, 25, 2499-2514

2. Need a better presentation and validation on the newly optimized key photosynthesis and stomatal conductance model parameters (i.e., V_{cmax} and m). Was it only revised for the flux sites (as presented in Figure 2)? How were they interpolated into the global scales and what are their uncertainties? How about the spatial and temporal variations of these parameters globally? Also, what will be the differences in the simulated GPP and ET between the new dynamic parameters and original fixed parameters in terms of accuracy and spatial pattern?

Thanks for the suggestion. As you are concerned, there are several problems that need to be addressed. This manuscript focuses on generating and sharing the reliable GPP and ET dataset. We included the global distributions of m and V_{cmax} in another paper which focuses on discussing the trend and spatial patterns of m and V_{cmax} (Leng et al., under review). However, we would add one chapter to include the spatial distributions, species distributions, and validations of m and V_{cmax} in this dataset manuscript to convince the readers on the accuracy and reliability of the dataset by Leng et al. (under review).

We included the validations of the Random Forest regressor for m and V_{cmax} estimations by courtesy of Leng et al. (under review), as shown in Figure 1. The Random Forest regressor estimates m and V_{cmax} with good agreements to the optimized m and V_{cmax} from measured fluxes in both the training sets and the validation set. The Random Forest regressor can estimate m with R^2 = 0.95 and RMSE = 1.414 in the training set (Figure 1a), and R^2 = 0.59 and RMSE = 3.663 in the independent validation set (Figure 1b). The Random Forest regressor can estimate V_{cmax} with R^2 = 0.98 and RMSE = 4.191 μmol m^{-2} s^{-1} (Figure 1c), and R^2 = 0.84 and RMSE = 10.598 μmol m^{-2} s^{-1} in the independent validation set (Figure 1d). Most of the scatter points locate beside the 1:1 line in both the training and validation set, showing the good accuracy of the Random Forest regressor for m and V_{cmax} estimation. The Random Forest regressors build the bridge that links m and V_{cmax} derived from measured fluxes to the gridded data that can be expanded to global coverage and long timeseries.

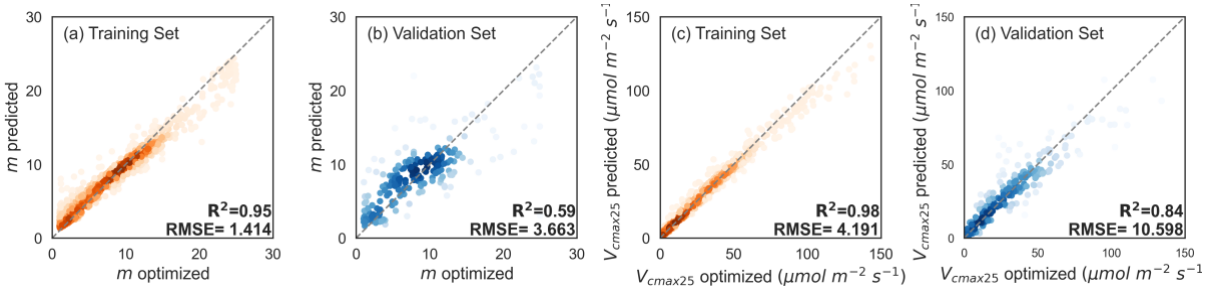

Figure 1. Comparisons of estimated m and V_{cmax25} from the Random Forest regressor and optimized m and V_{cmax25} from measured fluxes in the training set (a), (c) and in the independent validation set (b), (d) of the Random Forest Regressor, respectively. The color indicates the scatter density in each plot and the dotted lines indicate the 1:1 line in each plot.

Courtesy of Leng et al. (under review).

The global distributions of retrieved m and V_{cmax} are shown in Figure 2a and Figure 3a, and PFT-dependent patterns of m and V_{cmax} are observed in Figure 2b and Figure 3b. We also included the monthly spatial patterns of global m and V_{cmax} during 2001-2020 in Figure 4 and Figure 5, respectively. Strong seasonal variations in m and V_{cmax} are observed in boreal regions while m and V_{cmax} in subtropical and tropical regions are fairly constant within a year.

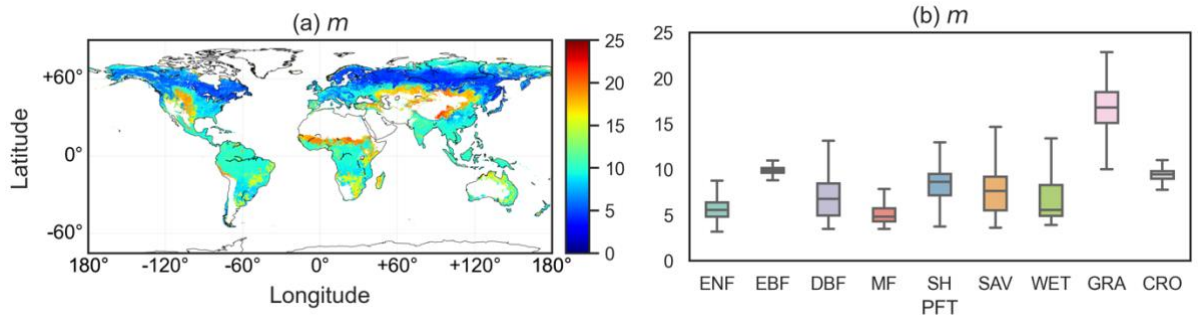

Figure 2. The spatial pattern of global m (a) and the averaged m in each PFT (b) during 2001-2020. Courtesy of Leng et al. (under review).

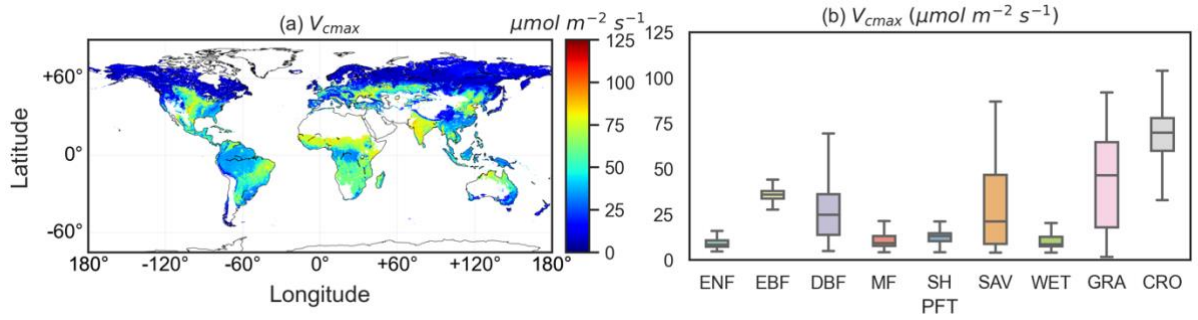

Figure 3. The spatial pattern of global V_{cmax} (a) and the averaged V_{cmax} in each PFT (b) during 2001-2020. Courtesy of Leng et al. (under review).

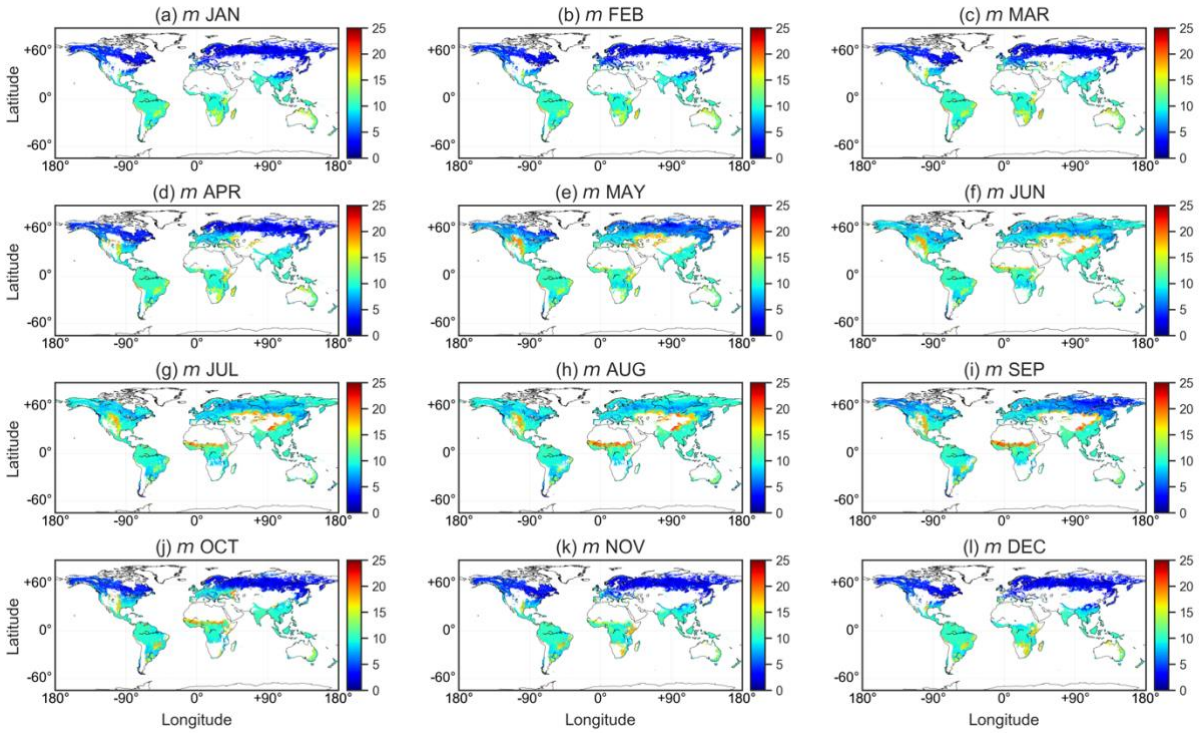

Figure 4. Monthly spatial patterns of global m during 2001-2020. (a) – (l) averaged m from January to December, respectively. Courtesy of Leng et al. (under review).

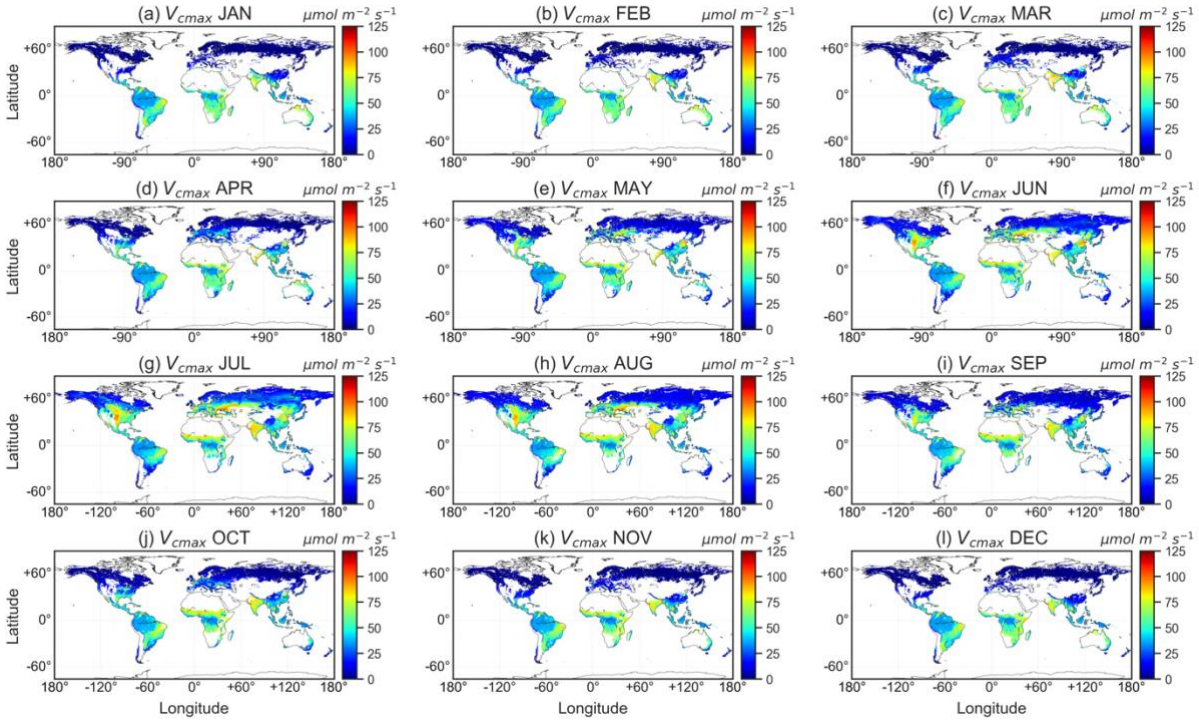

Figure 5. Monthly spatial patterns of global m during 2001-2020. (a) – (l) averaged m from January to December, respectively. Courtesy of Leng et al. (under review).

To further validate the gridded global m and V_{cmax}, we compared the global retrievals of m

and V_{cmax} in this study with the m census for various biomes from the review by Miner et al. (2017) and the V_{cmax} field measurements collected from Smith et al. (2019), as shown in Figure 6. m estimates in this study were compared with the mean and standard deviation in Miner et al. (2017) while V_{cmax} observations with the timestamp of measurement were compared with the estimated V_{cmax} in the corresponding time period in 2001-2020. Only 0.25° pixels with more than three V_{cmax} measurements were selected in the comparison. The estimated m in the global retrievals agrees well with the measured m, with $R^2 = 0.62$ ($P = 0.06$) and the estimated V_{cmax} in the global retrievals agrees well with the measured V_{cmax}, with $R^2 = 0.59$ ($P < 0.001$).

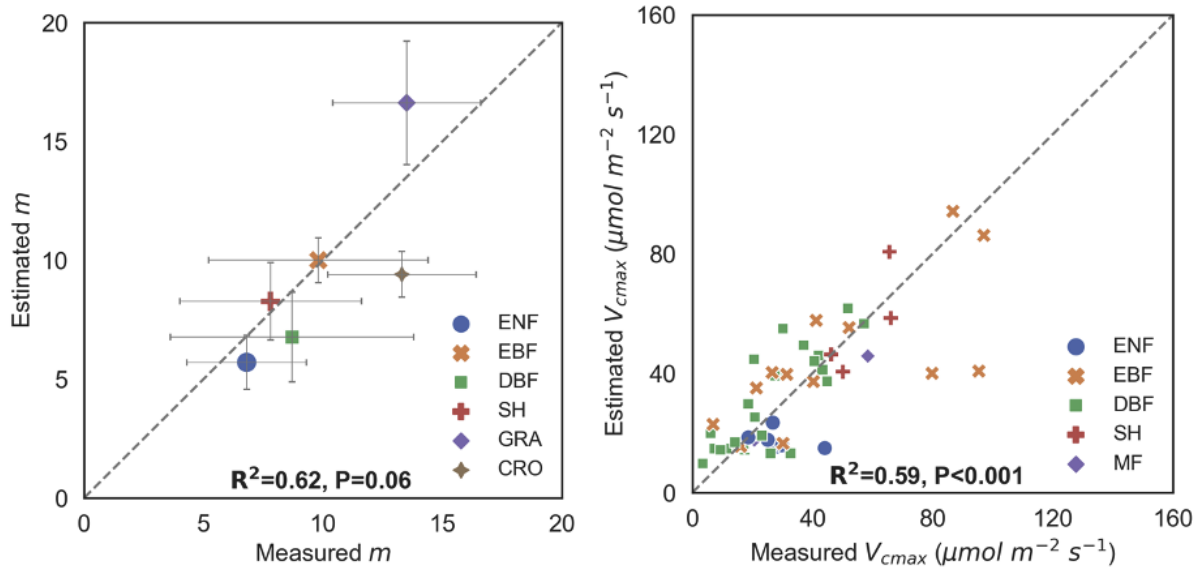

Figure 6. Left: Comparison between the PFT-scale mean values of estimated m from the Random Forest regressor and the measured m values reported in the review by Miner et al. (2017). Each horizontal and vertical bar represents the mean $m \pm 1$ standard deviation in the literature values and the estimated values, respectively. The sample sizes of measured m for each PFT are $n = 23$ (ENF), $n = 23$ (EBF), $n = 54$ (DBF), $n = 11$ (SH), $n = 5$ (GRA), and $n = 53$ (CRO). Right: Comparison between the PFT-scale mean values of predicted V_{cmax} from the Random Forest regressor and the measured V_{cmax} values reported in the review by Smith et al. (2019). Courtesy of Leng et al. (under review).

References:

Leng, J., Chen, J.M., Li, W., Luo, X., Xu, M., Rogers, C., Yan, Y.: Declining global sensitivity of stomatal conductance to photosynthesis. Submitted to *Global Change Biology* (under review)

Miner, G.L., Bauerle, W.L., & Baldocchi, D.D. (2017). Estimating the sensitivity of stomatal conductance to photosynthesis: a review. Plant, Cell & Environment, 40, 1214-1238

Smith, N.G., Keenan, T.F., Colin Prentice, I., Wang, H., Wright, I.J., Niinemets, U., Crous, K.Y., Domingues, T.F., Guerrieri, R., Yoko Ishida, F., Kattge, J., Kruger, E.L., Maire, V., Rogers, A., Serbin, S.P., Tarvainen, L., Togashi, H.F., Townsend, P.A., Wang, M., Weerasinghe, L.K., & Zhou, S.X. (2019). Global photosynthetic capacity is optimized to the environment. Ecological Letter, 22, 506-517

3. Figure 1. The bottom-up order is quite counter-intuitive to readers. Suggest using top-down order.

Thanks for the suggestion. We have revised the Figure 7 as the top-down order.

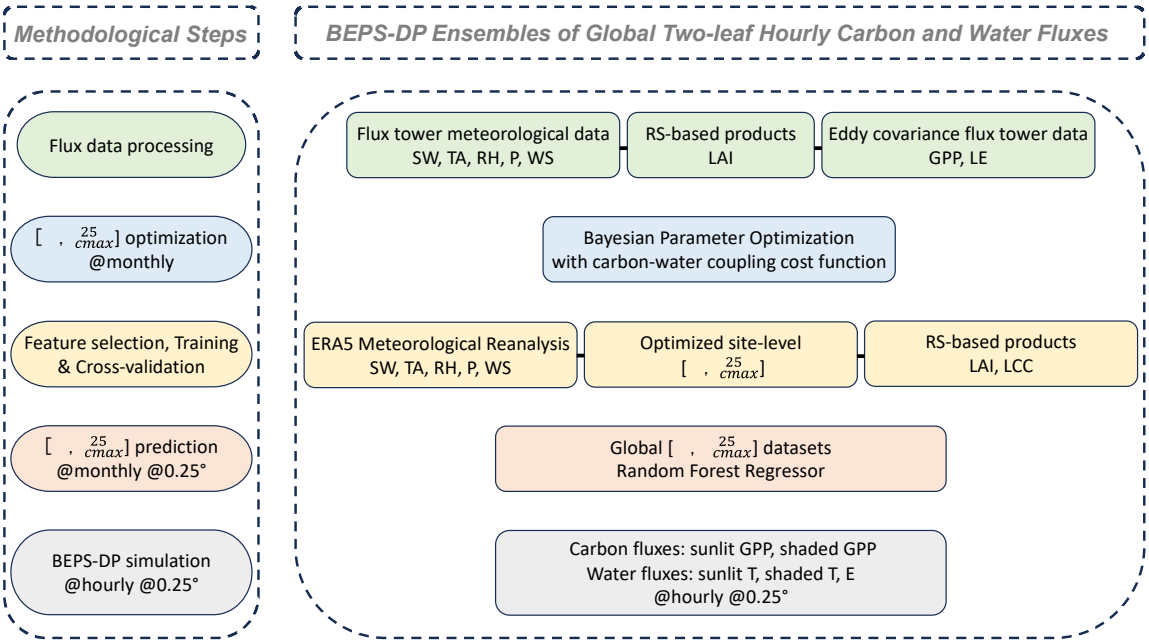

Figure 7. Schematic overview of the methodology and data products of the BEPS model with dynamic parameterizations (BEPS-DP). The flow diagrams show the methodological steps (left) and the details (right) for the BEPS-DP datasets of global hourly two-leaf carbon and water fluxes. SW (shortwave radiation, W m^{-2}), TA (air temperature, °C), RH (relative humidity, %), P (precipitation, mm h^{-1}), WS (wind speed, m s^{-1}), GPP (gross primary productivity, g C m^{-2} h^{-1}), LE (latent heat, W m^{-2}).

4. Figure 4, suggest adding the label of 1 in the slope subplots as a reference of good fitting.

Thanks for the suggestion. We have added the label of 1 in the slope and R^2 subplots as a reference of good fitting, as shown in Figure 8.

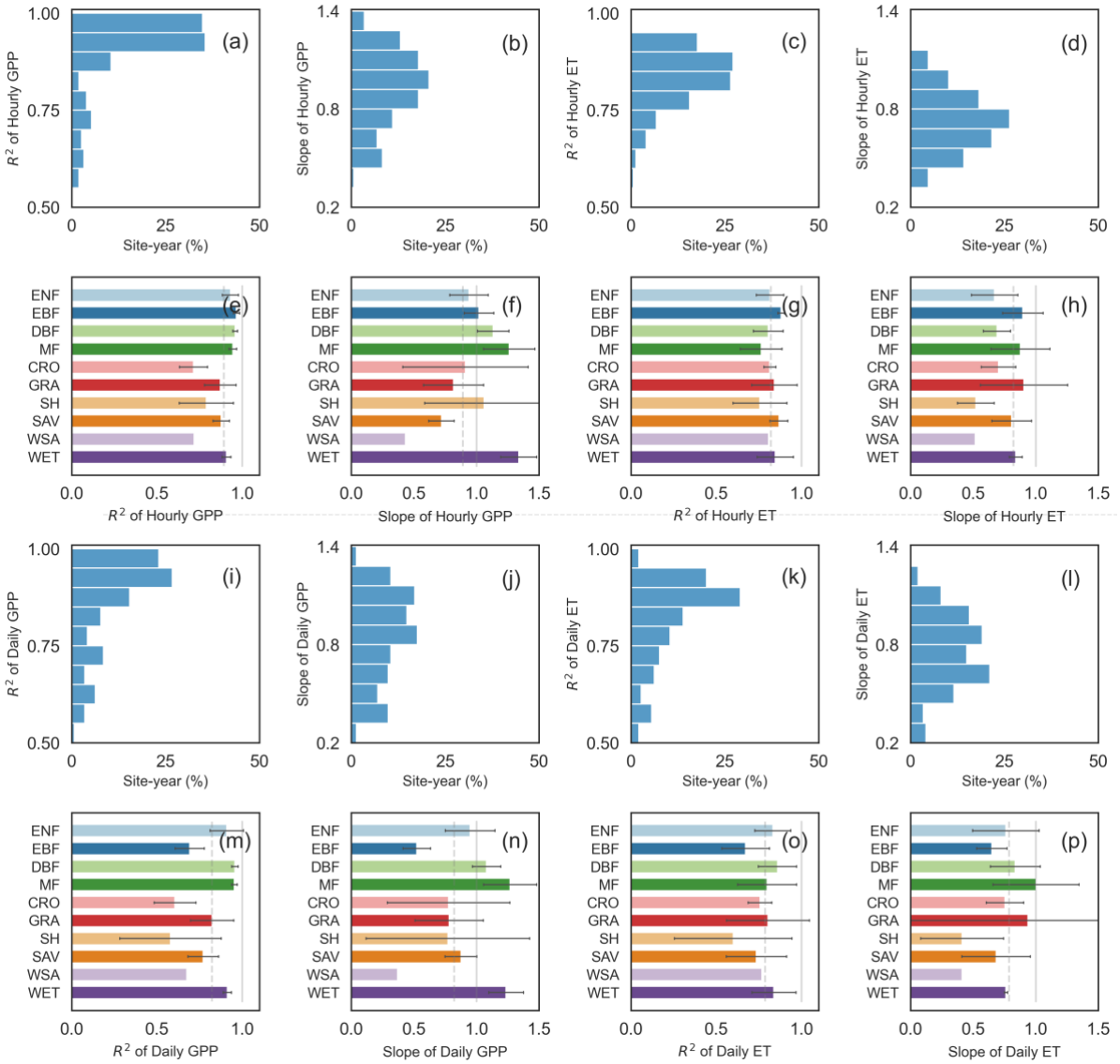

Figure 8. Evaluation of modeled hourly and daily fluxes against the eddy covariance data in the independent validation set: site-year percentage of R^2 in (a) hourly GPP; (c) hourly ET; (i) daily GPP; (k) daily ET; site-year percentage of regression slopes in (b) hourly GPP; (d) hourly ET; (j) daily GPP; (l) daily ET; the mean and standard deviation (SD) of R^2 in each PFT in (e) hourly GPP; (g) hourly ET; (m) daily GPP; (o) daily ET; the mean and standard deviation of regression slopes in each PFT in (f) hourly GPP; (h) hourly ET; (n) daily GPP; (p) daily ET. The grey lines indicate 1.0 in R^2 and regression slopes as a reference of good fitting. The dashed grey lines in (e) – (h) and (m) – (p) indicate the mean of R^2 and regression slopes for all PFTs in GPP and ET.

5. Need better presentations on the diurnal patterns of GPP and ET for different vegetation function types. For example, providing hourly curves for different vegetation function types and validated against flux site observations. It is still unclear whether these products can capture the diurnal variations of GPP and ET.

Thanks for your suggestions. Since there are 20% of all the sites (809 site years) in the

independent validation set for the comparisons of modeled and measured GPP and ET, it would be too redundant to show all the diurnal patterns (i.e., the hourly curves) for different vegetation functional types in the manuscript. However, for better presentations of our GPP and ET product simulated based on BEPS with dynamic parameterizations, we randomly selected one site-year per each PFT and showed the simulated GPP and ET against flux site observations in three different stages (i.e., day of year 115-125, 195-205, and 275-285). The sites and site-year we selected in the presentations of diurnal curves were shown in the table below.

Site Name	IGBP	Year	Lat	Lon
CH-Oe2	CRO	2013	47.2863	7.7343
US-KS2	SH	2004	28.6086	-80.6715
DE-Hai	DBF	2004	51.0792	10.4530
IT-Cpz	EBF	2003	41.7053	12.3761
DE-Tha	ENF	2004	50.9624	13.5652
NL-Hor	GRA	2008	52.2404	5.0713
JP-SMF	MF	2005	35.2617	137.0788
AU-Dry	SAV	2010	-15.2588	132.3706
CN-Ha2	WET	2003	37.6086	101.3269
US-Ton	WSA	2011	38.4316	-120.9660

The diurnal variations of simulated GPP and ET against flux observations were shown below, in three different stages per each site year (the beginning, peak, and ending of the growing seasons). The R^2 for GPP and ET in different stages per each site year were shown on the left-top in each subplot.

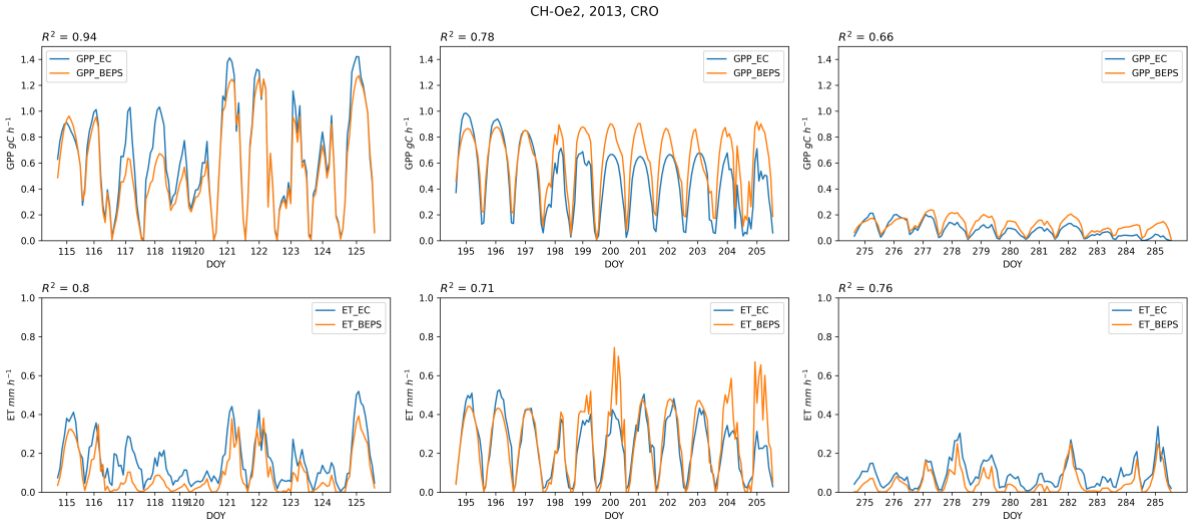

US-KS2, 2004, SH

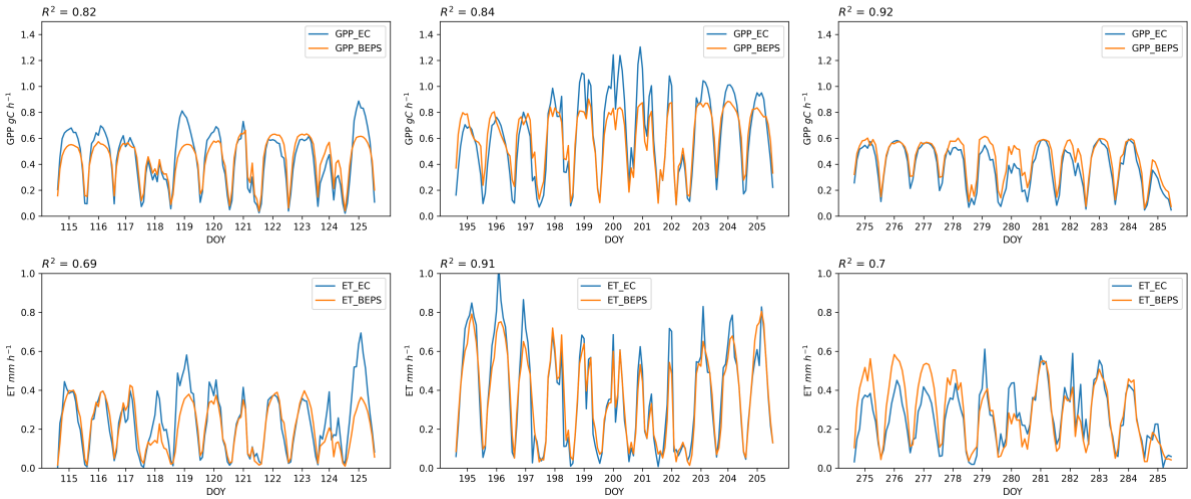

DE-Hai, 2004, DBF

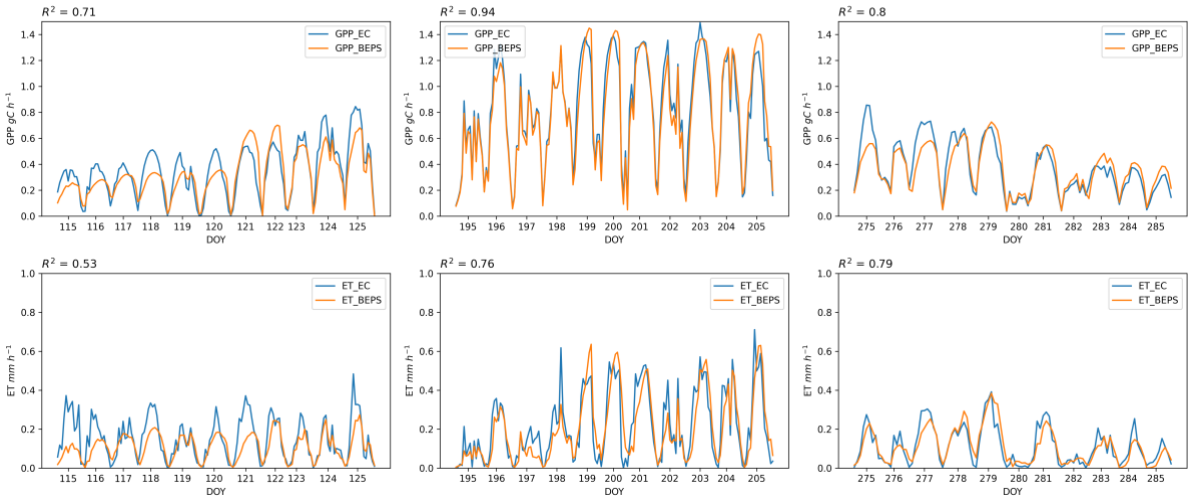

IT-Cpz, 2003, EBF

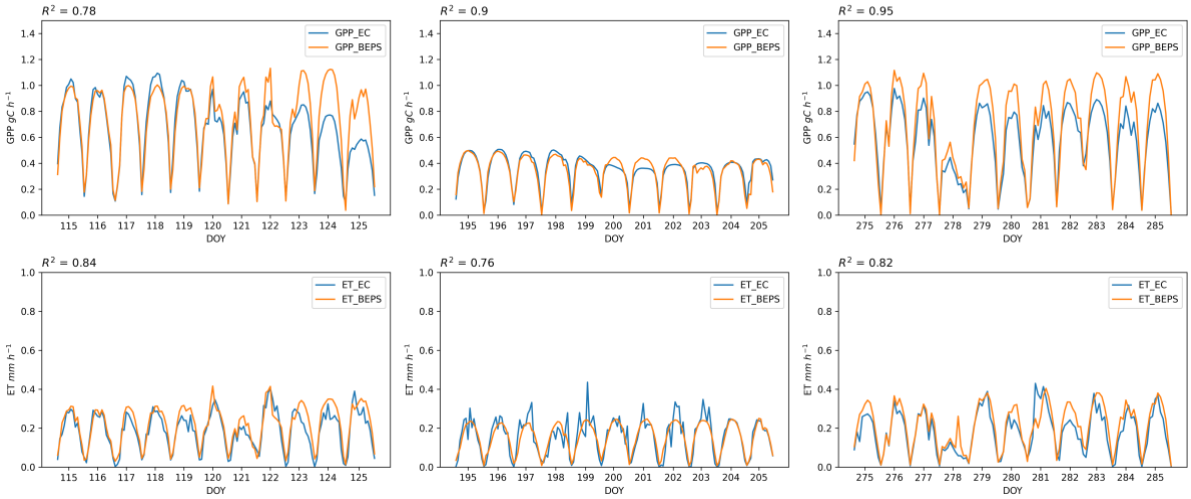

DE-Tha, 2004, ENF

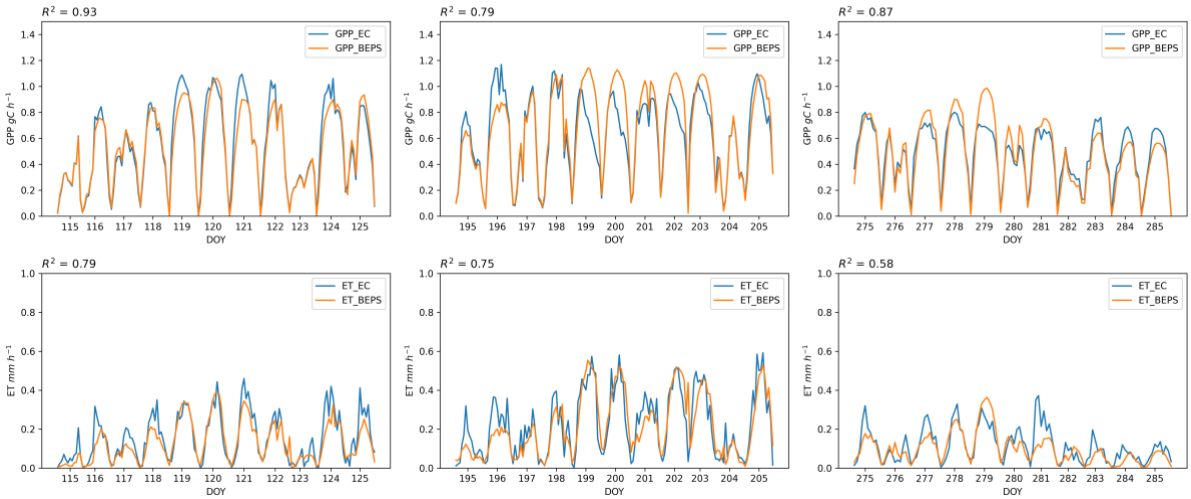

NL-Hor, 2008, GRA

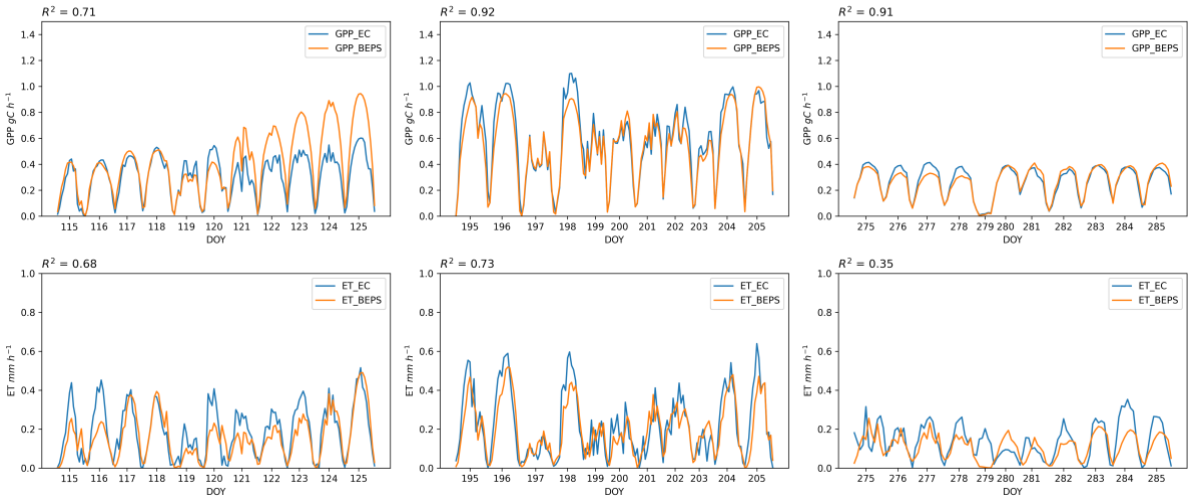

JP-SMF, 2005, MF

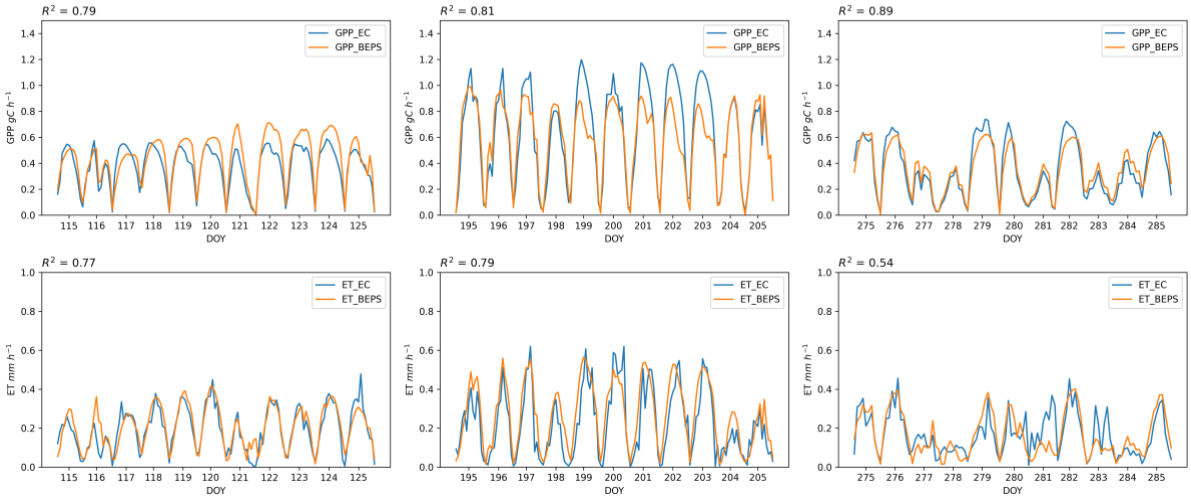

6. Dataset links update

Besides, we updated the link of dataset thanks to the National Ecosystem Data Bank for providing the platform for sharing the dataset. The updated links include the hourly two-leaf

GPP and ET dataset (3.3 TB) and the accumulated daily two-leaf GPP and ET dataset (197 GB) in 2001-2020. The corresponding paragraphs (Abstract, Code and Data Availability) in the manuscript was also updated.

"Abstract
... The hourly and accumulated daily GPP and ET estimates are available at https://doi.org/10.57760/sciencedb.ecodb.00163 (Leng et al., 2023a) and https://doi.org/10.57760/sciencedb.ecodb.00165 (Leng et al., 2023b)."

"Code and Data Availability
The 0.25°× 0.25° global hourly two-leaf GPP and ET datasets for 2001-2020 are available at https://doi.org/10.57760/sciencedb.ecodb.00163 (Leng et al., 2023a). The datasets are provided in NetCDF4 format. The GPP datasets include two components, the hourly GPP of sunlit and shaded leaves. The ET datasets include three components, the hourly evapotranspiration, transpiration of sunlit and shaded leaves. Each hourly NetCDF4 file represents the GPP/ET in a year at an hourly scale (g C m^{-2} h^{-1}/mm h^{-1}). The accumulated daily GPP and ET datasets for 2001-2020 are available at https://doi.org/10.57760/sciencedb.ecodb.00165 (Leng et al., 2023b). Each daily NetCDF4 file represents the GPP/ET in a year at a daily scale (g C m^{-2} d^{-1}/mm d^{-1}) ..."

References:

Leng, J., Chen, J.M., Li, W., Luo, X., Xu, M., Liu, J., Wang, R., Rogers, C., Li, B., Yan, Y., 2023a. Global Datasets of Hourly Carbon and Water Fluxes Simulated Using a Satellite-based Process Model with Dynamic Parameterizations [DS/OL]. V1. Science Data Bank. https://doi.org/10.57760/sciencedb.ecodb.00165. DOI: 10.57760/sciencedb.ecodb.00165.

Leng, J., Chen, J.M., Li, W., Luo, X., Xu, M., Liu, J., Wang, R., Rogers, C., Li, B., Yan, Y., 2023b. Global Datasets of Daily Carbon and Water Fluxes Simulated Using a Satellite-based Process Model with Dynamic Parameterizations [DS/OL]. V1. Science Data Bank. https://doi.org/10.57760/sciencedb.ecodb.00165. DOI: 10.57760/sciencedb.ecodb.00165.